Development 138, 1827-1838 (2011) doi:10.1242/dev.053645


# p53 coordinates cranial neural crest cell growth and epithelial-mesenchymal transition/delamination processes

**Ariel Rinon[1], Alina Molchadsky[2], Elisha Nathan[1], Gili Yovel[1], Varda Rotter[2], Rachel Sarig[1] and Eldad Tzahor[1,*]**

## SUMMARY

Neural crest development involves epithelial-mesenchymal transition (EMT), during which epithelial cells are converted into individual migratory cells. Notably, the same signaling pathways regulate EMT function during both development and tumor metastasis. p53 plays multiple roles in the prevention of tumor development; however, its precise roles during embryogenesis are less clear. We have investigated the role of p53 in early cranial neural crest (CNC) development in chick and mouse embryos. In the mouse, *p53* knockout embryos displayed broad craniofacial defects in skeletal, neuronal and muscle tissues. In the chick, p53 is expressed in CNC progenitors and its expression decreases with their delamination from the neural tube. Stabilization of p53 protein using a pharmacological inhibitor of its negative regulator, MDM2, resulted in reduced SNAIL2 (SLUG) and ETS1 expression, fewer migrating CNC cells and in craniofacial defects. By contrast, electroporation of a dominant-negative p53 construct increased PAX7$^+$ SOX9$^+$ CNC progenitors and EMT/delamination of CNC from the neural tube, although the migration of these cells to the periphery was impaired. Investigating the underlying molecular mechanisms revealed that p53 coordinates CNC cell growth and EMT/delamination processes by affecting cell cycle gene expression and proliferation at discrete developmental stages; disruption of these processes can lead to craniofacial defects.

**KEY WORDS: Cranial neural crest, Craniofacial development, Epithelial-mesenchymal transition, EMT, p53, Mouse, Chick**

## INTRODUCTION

The tumor suppressor p53 (Trp53), which has been referred to as the 'guardian of the genome', plays key roles in the prevention of tumor development (Lane, 1992); however, its precise roles during embryogenesis remain to be elucidated. Initial analyses of *p53* knockout mice showed no overt developmental defects, although these mice developed tumors within 6 months (Donehower et al., 1992). More recently, severe gastrulation defects have been observed in p53-deficient *Xenopus* embryos (Cordenonsi et al., 2003). It appears that repression of p53 is required to promote an ectodermal identity at the expense of a mesodermal cell fate (Sasai et al., 2008). In the mouse, the p53 family members p63 and p73 (Trp63 and Trp73) are expressed in early embryos and are likely to compensate for the loss of p53, whereas in frogs p53 is solely responsible for early embryogenesis (Stiewe, 2007).

In addition to the known functions of p53 in the prevention of tumor development by promoting growth arrest and apoptosis, growing evidence suggests that p53 also functions as a regulator of cell differentiation (Almog and Rotter, 1997; Zambetti et al., 2006). For example, cell culture studies have established that during myogenesis p53 plays a role in regulating the cell cycle and muscle gene expression (Cam et al., 2006; Molchadsky et al., 2008; Porrello et al., 2000; Soddu et al., 1996). Furthermore, p53 is involved in muscle stem cell behavior and muscle atrophy (Schwarzkopf et al., 2006).

[1]Department of Biological Regulation, Weizmann Institute of Science, Rehovot 76100, Israel. [2]Department of Molecular Cell Biology, Weizmann Institute of Science, Rehovot 76100, Israel.

*Author for correspondence (eldad.tzahor@weizmann.ac.il)

**Accepted 7 February 2011**

Several studies in the mouse have shown that some *p53* null embryos display diverse craniofacial abnormalities, such as exencephaly, which is a severe midbrain defect (Armstrong et al., 1995; Sah et al., 1995). As developmental processes and apoptosis are highly intertwined and p53 is a major regulator of apoptotic programs, it is highly likely that p53 deficiency would result in impaired development. Indeed, more recently, p53 was shown to play a major role in Treacher Collins syndrome (TCS), a congenital haploinsufficiency disorder in humans that arises from mutations in the *TCOF1* gene: in the absence of one *Tcof1* allele in the mouse, upregulation of p53-related apoptotic genes in neural crest progenitors leads to severe craniofacial defects (Jones et al., 2008). p53 and Mdm2 (a negative regulator of p53 and also its direct target) are expressed in the neural tube and in neural crest cells (Daujat et al., 2001; Krinka et al., 2001). Recently, it was shown that the homeodomain transcription factor Pax3 regulates neural tube closure, which is required for proper craniofacial development by inhibiting p53-dependent apoptosis (Morgan et al., 2008; Pani et al., 2002). Along these lines, it was previously shown in *Xenopus* that Pescadillo, a multifunctional nuclear protein involved in neural crest cell migration, inhibits p53 activity to prevent CNC apoptosis (Gessert et al., 2007).

Craniofacial development is a tightly orchestrated process that requires the contribution of various embryonic cell types. Cranial neural crest (CNC) cells give rise to most of the vertebrate skeletal system, including bones, cartilage and connective tissues in the face (Helms et al., 2005), whereas facial muscles originate from diverse head mesoderm lineages (Tzahor, 2009). CNC and mesoderm cells maintain intimate functional and regulatory relationships during craniofacial development (Trainor and Krumlauf, 2001). Head muscle precursors migrate into the branchial arches (BAs, also known as pharyngeal arches), which are the templates of the adult craniofacial structures. Within the BAs, CNC cells surround the muscle anlagen in a highly organized fashion (Noden, 1983a;

Noden, 1983b; Trainor and Tam, 1995). Mesoderm-derived muscle cells fuse in a highly coordinated manner to form a myofiber, which is attached to a specific CNC-derived skeletal element through CNC-derived connective tissue. CNC cells are thought to be involved in the patterning of the head musculature (Noden and Trainor, 2005). We previously demonstrated that head muscle patterning and differentiation are governed by the interaction of head muscle progenitors with the adjacent CNC cells (Rinon et al., 2007; Tzahor et al., 2003). Therefore, CNC cells impose anatomical features of the musculoskeletal architecture upon their neighbors (Grenier et al., 2009; Heude et al., 2010; Rinon et al., 2007; Tokita and Schneider, 2009).

Neural crest development and, in particular, the delamination of neural crest cells from the neural tube, involve an epithelial-mesenchymal transition (EMT), during which epithelial cells are converted into migratory mesenchymal cells (Sauka-Spengler and Bronner-Fraser, 2008). The dorsal neural folds contain pre-migratory CNC cells that express 'neural crest specifier' genes, such as members of the Sox and Snail families. Following EMT, and prior to their differentiation, these cells migrate to distinct regions of the developing embryo (Acloque et al., 2009). EMT is characterized by cytoskeletal changes, breakdown of the basement membrane, cell ingression and migration through the extracellular matrix (ECM). Thus, EMT causes cells to acquire invasive properties.

A key step in the initiation of CNC cell migration from the neural tube is the decrease in cell-cell adhesion that occurs when components of cell junction complexes, such as cadherins, are downregulated (Shoval et al., 2007; Taneyhill et al., 2007; Tucker et al., 1988). Currently, it is thought that cranial and trunk neural crest cells employ distinct subcellular mechanisms to initiate EMT, invade the ECM and migrate (Yang and Weinberg, 2008). Importantly, reactivation of the steps that lead to EMT during embryonic development is seen during tumor progression (Acloque et al., 2009; Le Douarin and Kalcheim, 1999; Yang and Weinberg, 2008). Hence, EMT is considered the first step in the metastatic cascade. The transcriptional repressors Snail (Snai1) and Snail2 (Slug or Snai2) contribute to cancer progression by mediating EMT, resulting in inactivation of p53-mediated apoptosis (Kurrey et al., 2009). A link between p53 and Snail2 has been established, such that Snail2 functions downstream of p53 in hematopoietic progenitors to circumvent p53-induced apoptosis (Wu et al., 2005).

In the present study, we used both mouse and chick models to study the role of p53 in craniofacial development. Analysis of *p53* null mouse embryos showed that both CNC-derived tissues (e.g. bones and sensory neurons) and skeletal muscles are mispatterned. In the chick, p53 is expressed in CNC progenitors, and its expression decreases with their delamination from the neural tube. To investigate the role of p53 in CNC progenitors, we performed both gain- and loss-of-function experiments. Stabilization of the endogenous p53 protein by Nutlin-3 (which inhibits MDM2 activity) or by electroporation of wild-type (wt) p53, reduced the expression of the CNC regulators *SNAIL2* and *ETS1* and, as a consequence, affected craniofacial development. Loss of p53 activity by the misexpression of a dominant-negative form of p53 in these cells resulted in elevated expression of the CNC markers PAX7, SOX9 and ETS1, presumably augmenting CNC progenitors in the neural tube. Notably, CNC cells failed to leave the neural tube. Furthermore, we provide evidence that p53 acts as a cell cycle/cell growth regulator in distinct CNC progenitor pools to fine-tune EMT-driven delamination. Our findings shed light on the dynamic, non-apoptotic roles of p53 during early CNC development.

## MATERIALS AND METHODS

### Chick embryos

Fertilized white eggs from commercial sources were incubated for 1-7 days at 38.5°C in a humidified incubator to Hamburger-Hamilton stage (St.) 3-30 (Hamburger and Hamilton, 1992).

### Whole-mount in situ hybridization

Whole-mount in situ hybridization was performed using digoxigenin (dig)-labeled antisense riboprobes synthesized from total cDNA as described (Harel et al., 2009; Tirosh-Finkel et al., 2006).

### Mouse lines

*Myf5-nlacZ* mice (*Myf5*$^{nlacZ/+}$) (Tajbakhsh et al., 1996) were bred and maintained on a C57B background. *p53* heterozygous mice were obtained from Jackson Laboratories and were used for creating *p53* knockout (*p53*$^{-/-}$) mice. All mice were maintained inside a barrier facility, and experiments were performed in accordance with Weizmann Institute of Science regulations for animal care and handling.

### Sectioning and immunohistochemistry

Embryos were fixed in 4% paraformaldehyde (PFA), embedded in paraffin and sectioned at 10-15 μm using a Leica microtome. For frozen sections, embryos were fixed with 4% PFA, washed and rocked overnight with 20-30% sucrose, embedded in OCT and sectioned at 10 μm using a Leica cryostat. Sections were blocked with 5% whole goat serum in 1% bovine serum albumin in PBS, prior to incubation with primary antibody. We used the following primary antibodies: BrdU (G3G4; 1:100), myosin heavy chain (MHC; MF20; undiluted), neurofilament (NF; 2H3; 1:20), Col2a (Col2a1; 1:40), Snail2 (1:20), Pax7 (undiluted) (all from DSHB, University of Iowa); phospho-histone H3 (pHIS3; 1:400), activated caspase 3 (1:50) (both from Santa Cruz Biotechnology); HNK1 (1:80; DSHB); chick p53 (undiluted; from V.R. lab); and Sox9 (1:1000; generous gift of Dr Robin Lovell-Badge, NIMR, London, UK). Cy2-, Cy3- and Cy5-conjugated anti-mouse or anti-rabbit IgG secondary antibodies (Jackson Labs) were diluted 1:100.

### Cell proliferation assay

Embryos grown in New cultures (see in ovo electroporation, below) were incubated to the indicated stage. Then, 100 μl 10 mM 5′-bromo-2′-deoxyuridine (BrdU) were added for 1 hour at 37°C and embryos fixed and processed for cryostat sectioning. Selected sections were washed with PBS, incubated in an HCL:PBS (1:7) solution for 30 minutes at 37°C, washed with 0.1 M borate buffer (pH 8.5) and immunostained with anti-BrdU as described above.

### Cell culture

Primary mouse embryonic fibroblasts were derived from *p53*$^{+/+}$ and *p53*$^{-/-}$ sibling embryos and maintained in DMEM supplemented with 10% fetal calf serum and antibiotics. For Nutlin-3 treatment, subconfluent cell cultures were treated with Nutlin-3 (Alexis Corporation) at a final concentration of 25 μM for 24 hours. The 10 mM stock solution was prepared in DMSO.

### Quantitative real-time PCR (QRT-PCR)

Total RNA was isolated using the RNeasy Kit (Qiagen) according to the manufacturer's protocol. A 2 μg aliquot of total RNA was reverse transcribed using MMLV reverse transcriptase (Promega) and random hexamer primers. QRT-PCR was performed using SYBR Green PCR Master Mix (Applied Biosystems) on an ABI 7300 instrument (Applied Biosystems). Values were normalized to an *Hprt* housekeeping control.

### In ovo electroporation, plasmids and pharmacological reagents

A New culture-based electroporation system using an ECM830 apparatus (BTX) was used to introduce the different plasmids (Nathan et al., 2008). For electroporation, we used two pulses of 6V for a duration of 25 milliseconds. In brief, St. 4-8 chick embryos were soaked with PBS on Whatman filter paper and then inserted between charged electrodes in a special chamber filled with buffer. Next, we microinjected the indicated vector using a capillary to the future CNC (St. 4) or the neural tube lumen (St. 8). Embryos were then placed in small nutrient agar plates and left to develop in the incubator to the desired developmental stage. In some cases,

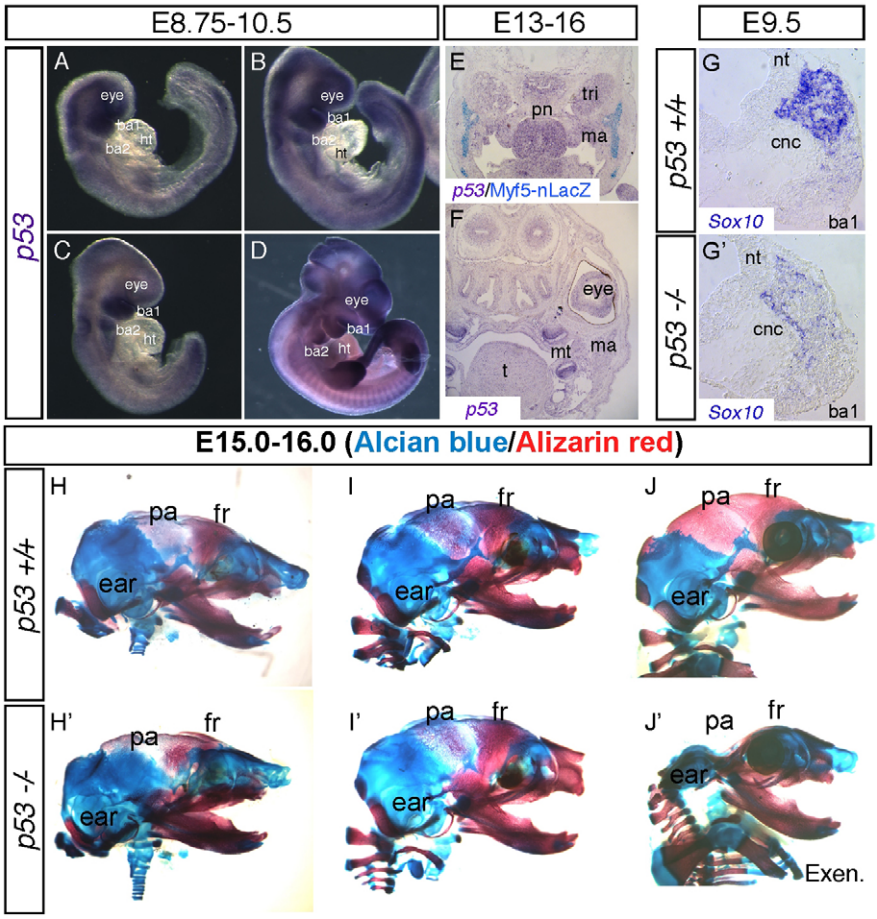


**Fig. 1. Loss of *p53* in the mouse results in embryonic craniofacial abnormalities.** (**A-D**) Whole-mount in situ hybridization for *p53* in E8.75-10.5 mouse embryos, showing that *p53* is expressed in the developing brain and in cranial neural crest (CNC) cells migrating into branchial arches 1-2. (**E**,**F**) Section in situ hybridization for *p53*. *Myf5* expression at E13 is marked by X-gal staining (blue) in *Myf5*$^{nlacZ/+}$ embryos. Note that *p53* is expressed outside the muscle anlagen at E13 (E), although at E16 it is faintly detected in head skeletal muscles [mastication (e.g. masseter) and extraocular muscles] (F) (see Fig. S1B-D in the supplementary material). (**G**,**G′**) Section in situ hybridization for *Sox10* on E9.5 mouse embryos. *Sox10* is substantially reduced in *p53* null embryos (*n*=3/3). (**H-J′**) Skeletal staining of E15-16 mouse embryos with Alizarin Red (bones) and Alcian Blue (cartilage). *p53* null embryos show diverse changes in their skeletal development compared with wild-type embryos. Note the reduction in frontal (fr; H′; *n*=2/8) and parietal (pa; I′; *n*=6/6) bone mass and their complete loss in exencephaly (Exen) mutants (J′; *n*=3/3). Lateral views (A-D,H-J), frontal sections (E,F) and transverse sections (G,G′) are shown. ba, branchial arch; ht, heart; pn, paranasal; tri, trigeminal ganglia; ma, masseter; mt, molar tooth; t, tongue; nt, neural tube.

GFP was targeted to one side, while the contralateral side served as an internal control. In the gain-of-function experiments, wt p53 and 10 mM Nutlin-3 (the pharmacological inhibitor of Mdm2) were used; DMSO was used as a control reagent at the same dilution (0.25%). A human wt *p53* sequence was PCR amplified and cloned using *Bam*HI sites into a pCAAGS-GFP-based vector (pCAB). The DNA sequence encoding the putative N-terminus of p53 was PCR amplified and subcloned using *Xho*I and *Cla*I sites into a pCAAGS vector to create DNp53.

### Time-lapse microscopy

An assembled inverted fluorescent microscope (Nikon ECLIPSE 90i) with a cooled CCD camera and a semi-automated temperature-controlled chamber was coupled with a software-controlled acquisition system (Image-Pro AMS version 6.0; Media Cybernetics). Captured images were analyzed by Adobe Photoshop and Image-Pro AMS software.

### Skeletal preparation

Cartilage and bones of mouse embryos were visualized after staining with Alcian Blue and Alizarin Red S, respectively (Sigma); clarification of soft tissues was obtained using KOH.

### Statistical analysis

Data were analyzed using Student's *t*-test to compare two groups. The results are presented as mean ± s.e.m.

## RESULTS

### *p53* null mouse embryos display musculoskeletal craniofacial abnormalities

It has been reported that a small percentage of *p53* null embryos suffer from abnormal craniofacial development (Armstrong et al., 1995; Donehower et al., 1992), although the skeletal muscle phenotype of these mutants has not been thoroughly investigated. To clarify whether p53 is involved in patterning the craniofacial musculoskeletal system in the mouse, we first performed in situ hybridization for *p53* during embryogenesis at E8.75-16, and revealed its prominent expression in CNC-derived tissues (Fig. 1A-D). Next, we analyzed *p53* expression at E13-16 in the myogenic reporter mouse line *Myf5*$^{nlacZ/+}$ (Tajbakhsh et al., 1996) to follow its expression in muscle progenitors. *p53* was predominantly expressed in CNC cells and in various CNC-derived tissues, such as the sensory ganglia primordia (Fig. 1E) and molar teeth (Fig. 1F). By contrast, *p53* expression in head muscles (e.g. eye muscles and masseter) was hardly detectable (see Fig. S1 in the supplementary material).

Because Sox genes are major regulators of craniofacial development (Hong and Saint-Jeannet, 2005), we first examined *Sox9* (data not shown) and *Sox10* expression in control and *p53* null mouse embryos. *Sox10* was significantly downregulated in *p53* mutants, suggesting that CNC development was altered in these mutants (Fig. 1G,G′). In contrast to the Sox genes, the expression of *Twist* and *Zeb2* (RNA) and Pax7 (protein), as well as the levels of the proliferation marker phosphohistone H3, were not significantly changed in the *p53* null mouse embryos (data not shown).

To gain additional insights into craniofacial development, we examined skeletal elements (bones and cartilage) in control versus *p53* null embryos (including those with exencephaly phenotypes). Alcian Blue/Alizarin Red staining for cartilage and bone was performed at E15-16. In *p53* null embryos, we observed a reduction in the mass of the frontal and parietal bones (red staining); these two bones were completely lost in the exencephaly

mutant (Fig. 1H-J′). We also found abnormal patterning of the sensory ganglia surrounding the extraocular muscles, as revealed by immunostaining for cranial sensory neurons (see Fig. S1 in the supplementary material). We next examined head muscle patterning in *p53* null embryos at E15-16, again observing varying degrees of patterning defects, including MHC expression in the extraocular muscles around the eye and within the mastication muscles (see Fig. S1 in the supplementary material). In summary, our detailed craniofacial examination of *p53* null embryos uncovered broad, albeit subtle, patterning defects in neuronal, skeletal and muscle tissues in the mouse.

## *p53* is expressed in neural crest progenitors in the chick

The subtle craniofacial defects in the neural crest and muscle lineages in *p53* mutants might reflect a low penetrance resulting from the genetic robustness of embryogenesis in mammals. To further explore the function of p53 in vertebrates, we utilized the avian embryonic system, in which defined spatial and temporal manipulations might reveal novel functions of this protein. To this end, we performed whole-mount in situ hybridization and immunohistochemistry on transverse sections of St. 8-11 chick embryos (Figs 2 and 3). *p53* and *CDM2* (a chick *Mdm2* homolog) were expressed in the developing neural tube, including its most dorsal tips, where CNC cells reside (Fig. 2; note the expression of the known CNC markers *SNAIL2*, *SOX9* and *ETS1*). At later stages (after St. 10), a gradual decay of *p53* was observed in the midbrain-forebrain region, at the dorsal neural tube (Fig. 2D). Hence, *p53* is downregulated in CNC cells, whereas *SNAIL2*, *SOX9* and *ETS1* are highly expressed when CNC cells delaminate and migrate from the neural tube to the periphery (Fig. 2D-T).

Immunostaining for p53 protein confirmed that it is expressed at the dorsal tips of the neural tube (Fig. 3C,G,G′), whereas SOX9 is restricted to the CNC (Fig. 3B,F,F′). p53 expression was considerably reduced in migrating CNC cells (Fig. 3C,G,G′), although some of these cells expressed both SOX9 and low levels of p53 (Fig. 3D,H,H′). These observations in the chick prompted us to investigate a possible role for p53 during early CNC formation.

## Upregulation or stabilization of p53 in the cranial neural tube reduces CNC delamination and promotes neural tube defects in chick embryos

The downregulation of p53 in migrating CNC cells (Figs 2 and 3) suggested that the inhibition of p53 is crucial for their delamination and/or migration to the periphery. We therefore tested whether increased p53 levels would affect these processes, utilizing the electroporation technique to misexpress wt p53. Since p53 regulates distinct cellular processes (e.g. cell cycle arrest and/or apoptosis), we first titrated the plasmid concentration to avoid growth and apoptotic defects (data not shown). Overexpression of p53 at these stages resulted in a reduction in the number of CNC cells migrating to the first BA, as compared with GFP-electroporated control embryos (data not shown). Furthermore, wt p53 repressed *ETS1* expression (see Fig. S2A in the supplementary material).

Since we observed increasing amounts of apoptotic cells within the neural tube upon wt p53 electroporation (data not shown), we next stabilized the protein at St. 8-13 using Nutlin-3, a well-defined pharmacological inhibitor of CDM2 binding to p53 (Vassilev, 2007) (Fig. 4). As a consequence, the p53 protein was stabilized in both the neural tube and in delaminating CNC cells of Nutlin-3-treated embryos, as evidenced by the elevated levels of p53 staining (Fig. 4A′, quantified in 4D) compared with DMSO-treated


**Fig. 2. Expression of *p53* and *CDM2* in CNC cells in the chick.** (**A-T**) Whole-mount in situ hybridization was performed in St. 8-11 chick embryos. *p53* and *CDM2* (a chick homolog of mouse *Mdm2*) are expressed in the neural tube and CNC (arrowheads). At St. 10-11, *p53* levels are decreased in the neural tube and in migrating CNCs (D) and *CDM2* is increased (H). Early CNC regulators (*Snail2*, *Sox9* and *Ets1*) at the different stages are shown for comparison (I-T). Dashed black lines demarcate the delamination of CNCs to the periphery. Dorsal views, anterior to the top. cnc, cranial neural crest; fb, forebrain; mb, midbrain; hb, hindbrain.

controls (Fig. 4A). Importantly, apoptosis was not induced in Nutlin-3-treated embryos (data not shown). Whereas immunostaining indicated comparable amounts of SOX9 in control and treated embryos, SNAIL2 was downregulated in response to Nutlin-3-induced p53 stabilization (Fig. 4B-C′, quantified in 4D′).

Next, we used in situ hybridization to test how the stabilization of p53 affected *SNAIL2* and *ETS1* expression (Fig. 4E-I′ and see Fig. S3 in the supplementary material). SNAIL2, a known regulator of EMT (Nieto, 2002), was recently shown to function in tandem

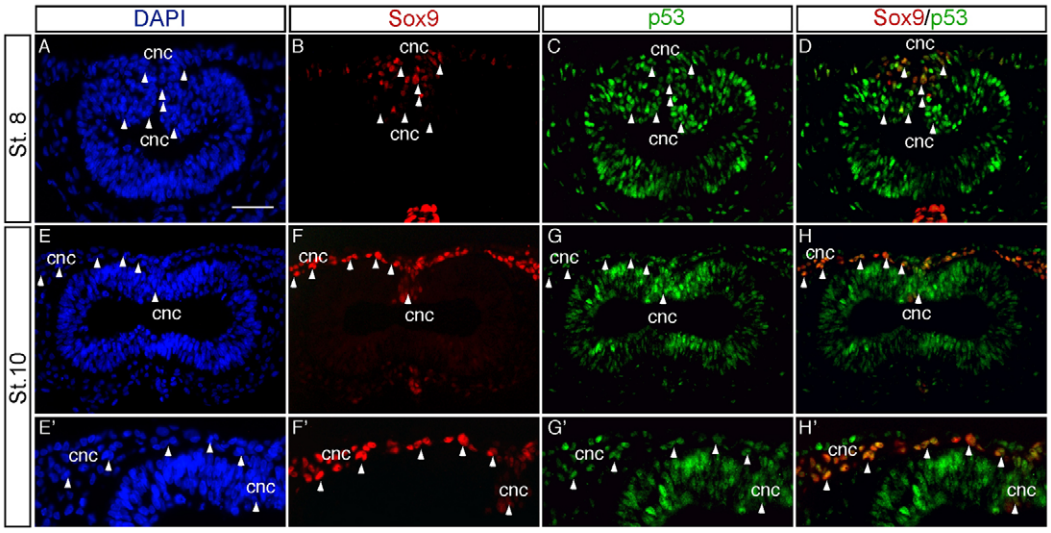


**Fig. 3. p53 protein is downregulated in delaminating CNC cells in the chick.** (**A-H′**) Transverse sections at St. 8-10 immunostained with Sox9 (red) and p53 (green) antibodies. At St. 8, p53 is expressed extensively in the neural tube (nt) and in the future CNC cells (co-localization of Sox9 and p53, yellow staining in D; arrowheads). At St. 10, p53 levels are downregulated or declining in delaminating CNC cells (F-H, arrowheads; higher magnification in F′-H′). DAPI staining (A,E,E′, blue) marks nuclei. cnc, cranial neural crest. Scale bar: 50 μm.

with ETS1 to enable delamination of neural crest cells from the neural tube, specifically in the head region (Theveneau et al., 2007). We noted that the levels of stabilized p53 at St. 8-9 did not affect the expression of *SNAIL2* (Fig. 4E′) and *ETS1* (data not shown). At later stages (after St. 9), however, p53 stabilization caused a gradual reduction in the mRNA levels of these genes (Fig. 4F-I′ and see Fig. S2 in the supplementary material).

RT-PCR analysis revealed a slight reduction in the CNC markers *SOX10*, *PAX7*, *SNAIL2* and *TWIST* in Nutlin-3-treated neural tubes versus those of control (DMSO-treated) embryos (Fig. 4J). Next, we explored the long-term consequences of a reduction in *SNAIL2* and *ETS1* for craniofacial development in E6-7 chick embryos following treatment with Nutlin-3. These embryos were characterized by major defects in neural tube closure, brain and eye development and overall growth compared with controls (Fig. 4K). By contrast, trunk regions, including the fore- and hindlimbs, developed largely normally. Furthermore, Nutlin-3-treated embryos displayed muscle patterning and differentiation defects compared with DMSO-treated controls (see Fig. S3 in the supplementary material). In these experiments, we detected hardly any changes in cartilage-derived CNC elements [e.g. in the interorbital septum and Meckel's cartilage (immunostained in red) and in the ECM protein collagen 2a (COL2A) (see Fig. S3 in the supplementary material)]. These findings in the chick suggest that p53 negatively regulates SNAIL2/ETS1 during neural tube closure stages. We suggest that p53 levels in CNC progenitors are reduced to allow SNAIL2/ETS1-dependent CNC delamination from the neural tube.

## Dominant-negative p53 affects CNC proliferation, delamination and migration

In order to gain further insights into the molecular mechanism underlying p53 involvement in CNC development in the chick, we used a dominant-negative form of p53 (DNp53) (Ossovskaya et al., 1996) that lacks its oligomerization domain, thereby inhibiting the DNA-binding activity of the endogenous protein. The p53 loss-of-function effect of this construct was demonstrated in a *p21* (*Cdkn1a*) promoter assay in WI-38 human lung fibroblasts as well as by its attenuation of p53-dependent apoptosis in vivo (see Fig. S4 in the supplementary material).

To investigate the role of p53 in CNC development, we electroporated DNp53 into St. 3-4 chick embryos and analyzed them at St. 11 (Fig. 5). Strikingly, the number of $PAX7^+$ and $SOX9^+$ cells was doubled in the DNp53-electroporated half of the neural tube (green) and in migrating CNC cells, as compared with the contralateral side (Fig. 5A-F, quantified in 5G). The results of further experiments to test whether the increase in $PAX7^+$ and $SOX9^+$ cells affects CNC specification or proliferation were consistent with increased cell proliferation induced by DNp53 (Fig. 5H-M, quantified in 5N). This result is consistent with the fact that SNAIL2 (mRNA and protein) expression levels were unchanged (data not shown).

To test how the increase in cell proliferation caused by DNp53 might affect CNC delamination and migration, we electroporated DNp53 into St. 9 embryos (Fig. 6). *ETS1* was upregulated in the dorsal neural tube, compared with control embryos (arrowheads in Fig. 6A-D′). These findings indicate that although CNC cells seem to initiate EMT (PAX7, SOX9 and ETS1 expression), they lack the ability to migrate from the neural tube. To further explore the dynamic migratory behavior of CNC cells in vivo, we used time-lapse microscopy. This dynamic live cell analysis corroborated our findings that a large proportion of midbrain-forebrain CNC cells fail to delaminate from the neural tube upon DNp53 electroporation, as compared with control GFP-electroporated embryos (Fig. 6E-H′). Whereas all GFP-labeled control cells left the neural tube within 7 hours post-electroporation, many of those that were electroporated with DNp53 remained trapped in the dorsal neural tube (compare Fig. 6H with 6H′).

Taken together, this loss-of-function approach uncovered possible roles for p53 in the coordination of CNC delamination (*ETS1* expression) and/or migration (time-lapse analysis), although we cannot distinguish between these cellular activities. These dynamic regulatory roles for p53 in early CNC development could account for the onset of craniofacial defects in the *p53* mutants.

## p53 coordinates cell cycle progression at the onset of CNC delamination

To gain further insights into the role of p53 during neural crest development, we focused on its effects on cell growth. We first investigated the proliferative state of epithelial cells (~St. 8) and delaminating CNC cells (~St. 10; see Fig. S5 in the supplementary material). Although it has been shown that trunk neural crest cells should be synchronized in S phase in order to delaminate from the posterior neural tube (Burstyn-Cohen et al., 2004), we found no

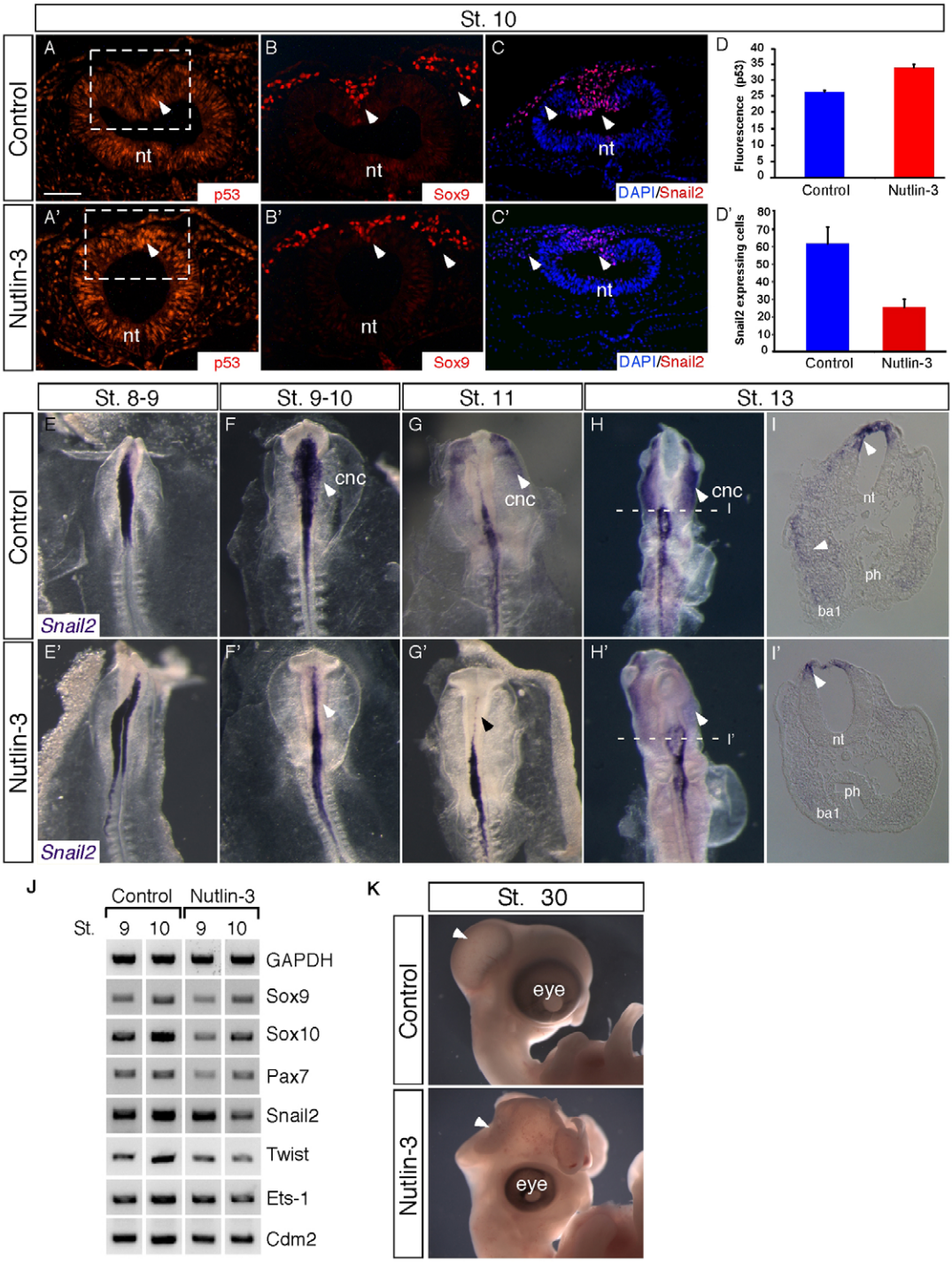


**Fig. 4. Stabilization of p53 protein by Nutlin-3 reduces SNAIL2 expression, CNC delamination and promotes craniofacial defects in the chick.** (**A**,**A'**) p53 immunostaining (red) at St. 10 after administration of Nutlin-3, as compared with control embryos treated with DMSO. (**B-C'**) Staining for SOX9 and SNAIL2 (red) in control and Nutlin-3-treated embryos (*n*=4/4). Arrowheads indicate delaminating and migrating CNC cells. The boxed region marks that quantified in D. (**D**,**D'**) Quantification of p53 protein fluorescence intensity (D, *P*<0.01) and the number of SNAIL2-expressing cells (D', *P*<0.01) in Nutlin-3-treated and control embryos. Error bars indicate s.e.m. D, *n*=3/5; D', *n*=4/6. (**E-H'**) *SNAIL2* in situ hybridization in St. 8-13 chick embryos after Nutlin-3 or DMSO administration. A reduction in *SNAIL2* expression is seen only at St. 10-13 in Nutlin-3-treated embryos (F'-H', white arrowheads; *n*=16/21). Arrowheads show reduced *SNAIL2* expression in Nutlin-3-treated embryos. (**I**,**I'**) Transverse sections (dashed lines in H,H') of St. 13 embryos in the head region, showing a reduction in *SNAIL2* (compare at arrowheads) in the neural tube and in migrating CNCs in Nutlin-3-treated embryos. (**J**) Semi-quantitative RT-PCR analysis of various neural crest genes in chick St. 9-10 neural tube. In Nutlin-3-treated embryos reduced *SOX10*, *SNAIL2*, *TWIST*, *PAX7* and *ETS1* is observed, as compared with control (DMSO-treated) embryos (*n*=3). (**K**) Long-term craniofacial phenotype at St. 30 of Nutlin-3-treated chick embryos (*n*=3/3). Arrowhead indicates a neural tube closure defect. A detailed analysis of these defects is shown in Fig. S4 in the supplementary material. In situ images are dorsal side up, anterior to the top; transverse sections (A-C) and lateral views (K) are shown. ba, branchial arch; cnc, cranial neural crest; nt, neural tube; ph, pharynx. Scale bar: 100 μm.

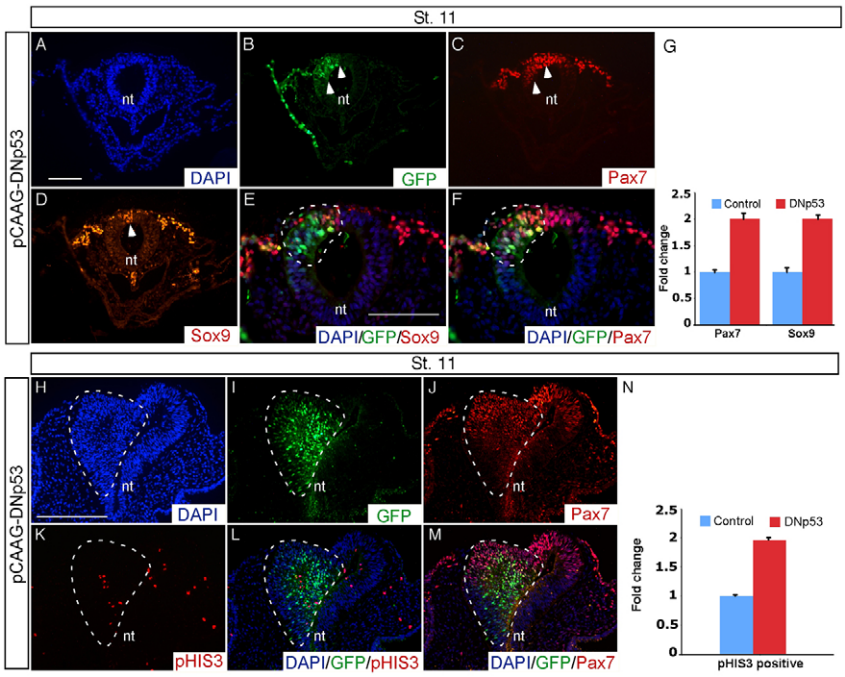


**Fig. 5. DNp53 electroporation upregulates PAX7 and SOX9 in CNC cells and CNC cell proliferation in the chick.** (**A-F**) Electroporation of dominant-negative p53 (DNp53, green by GFP) in St. 3-4 chick embryos followed by immunostaining shows a twofold increase in SOX9$^+$ and PAX7$^+$ cells within the neural tube (left, circled) as compared with the intact contralateral side (right). Arrowheads indicate electroporated (GFP$^+$) cells. DAPI staining (blue) marks nuclei. (**G**) Quantification of experiments shown in A-F. Error bars indicate s.e.m. *n*=4/4. (**H-M**) Electroporation DNp53 (GFP, green) in St. 3-4 chick embryos shows a twofold increase in neural crest proliferation within the neural tube (left, circled) as compared with intact contralateral side (right). Cell proliferation was assessed by immunostaining for the mitotic marker phosphohistone H3 (pHIS3, red). (**N**) Quantification of experiments shown in H-M. Error bars indicate s.e.m. *n*=3/3. nt, neural tube. Scale bars: 100 μm.

such indication for CNC progenitors. Furthermore, it was shown recently that only a fraction of CNC cells proliferate at the delamination/EMT stages (Theveneau et al., 2007). We observed increased numbers of proliferating cells between St. 8 and St. 10, coupled with increasing levels of SOX9 and SNAIL2 (see Fig. S5 in the supplementary material).

Next, we studied the effect of Nutlin-3 on the proliferation status and delamination/EMT of CNC cells (Fig. 7). Nutlin-3 treatment resulted in a reduction of BrdU$^+$ CNC cells and delaminating cells (~22%), consistent with the downregulation of SNAIL2 (Fig. 7A-E; see also Fig. 4C′,D′). To clarify these findings, we performed gene expression analyses for several cell cycle regulators by in situ

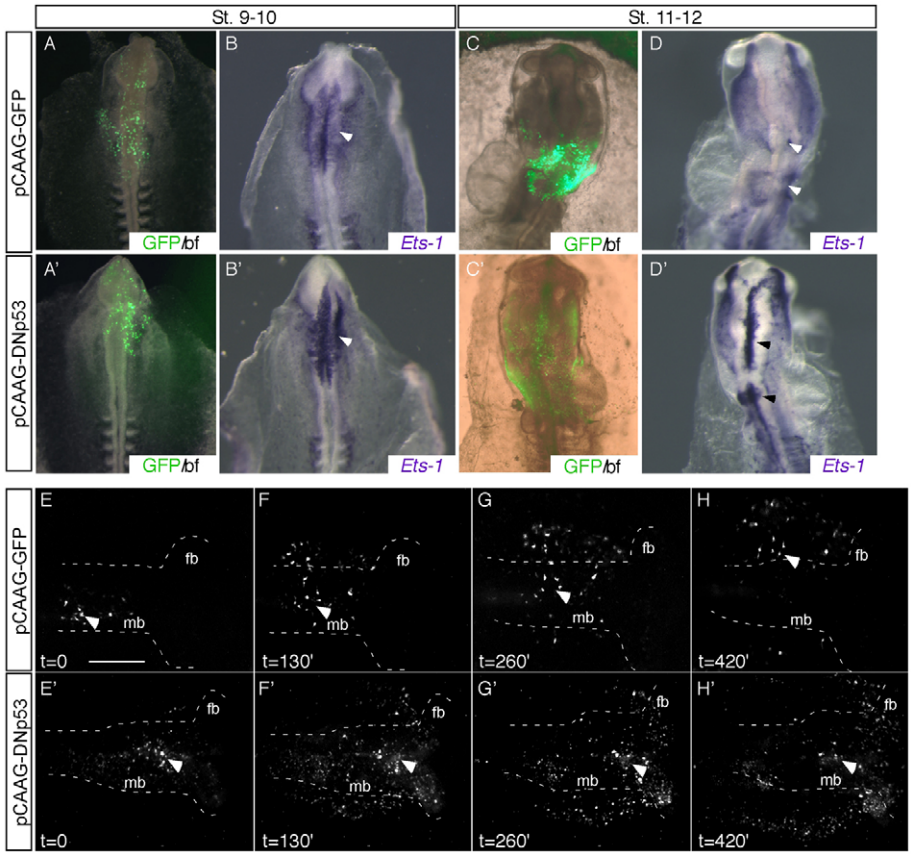


**Fig. 6. DNp53 electroporation upregulates *ETS1* in CNC cells and reduces their delamination from the chick neural tube.** (**A-D′**) Whole-mount in situ hybridization for *ETS1* (arrowheads) in St. 8 chick embryos after DNp53 electroporation (A′,B′,C′,D′; *n*=5/7) as compared with control GFP electroporation (A-D). Dorsal views, anterior to the top. (A,A′,C,C′) An overlay of GFP and bright-field (bf) images. (**E-H′**) Time-lapse analysis of GFP and DNp53 electroporations in CNC cells in St. 8 chick embryos. Note that some DNp53$^+$ cells (GFP, white) failed to delaminate from the midbrain-forebrain region during the experiment (420 minutes; arrowheads in E′,F′,G′,H′; *n*=5), as compared with the complete delamination and migration of control cells (arrowheads in E-H; *n*=4). Dorsal views, anterior to the right. mb, midbrain; fb, forebrain. Scale bar: 100 μm.

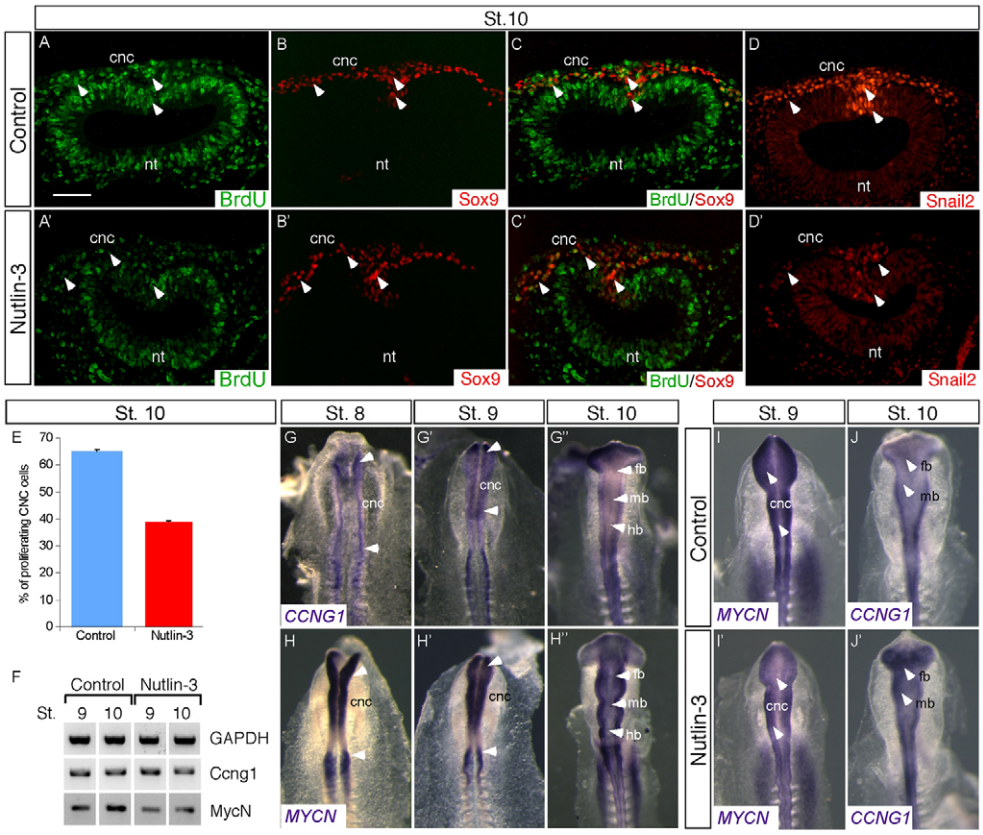


**Fig. 7. Stabilization of p53 reduces CNC proliferation.** (**A-E**) Immunostaining of transverse sections of chick neural tube at St. 10 for BrdU (green; marks cell proliferation), SOX9 (red) and SNAIL2 (red) after administration of Nutlin-3. Note the reduction in proliferating cells (E, ~22%; $P<0.05$) within the neural tube and delaminating CNC cells (arrowheads in A′), as compared with the DMSO-treated control embryos (A). SOX9 levels seem to be maintained whereas SNAIL2 was downregulated by Nutlin-3 (B′-D′ versus B-D). (C,C′) An overlay of BrdU and SOX9 co-staining. Error bars indicate s.e.m. E, $n=3/4$. (**F**) Semi-quantitative RT-PCR analysis of *CCNG1* and *MYCN* expression in chick St. 9-10 neural tube ($n=3$). (**G-H″**) Whole-mount in situ hybridization was performed for *CCNG1* and *MYCN*, showing their expression pattern within the developing neural tube and CNC cells (arrowheads). (**I-J′**) Downregulation of *MYCN* at St. 9 (I′, arrowheads) and upregulation of *CCNG1* at St. 10 (J′, arrowheads) by Nutlin-3 treatment, as compared with DMSO-treated control chick embryos (I,J). Dorsal views, anterior to the top. cnc, cranial neural crest; fb, forebrain; mb, midbrain; hb, hindbrain. Scale bar: 100 μm.

hybridization and RT-PCR. At St. 8-10, *p21*, *p27* (*CDKN1B*), cyclin D1 (*CCND1*) and cyclin D2 (*CCND2*) could hardly be detected (data not shown); however, cyclin G1 (*CCNG1*), which is known to be a p53 target (Jones et al., 2008), and *MYCN* were found to be expressed during these stages (Fig. 7G-H″). Stabilization of p53 in CNC cells slightly upregulated *CCNG1* and reduced *MYCN* expression (Fig. 7F,I′,J′). Collectively, these findings suggest that p53 coordinates cell cycle progression with EMT in CNC progenitors.

In order to obtain a general and unbiased view of the potential involvement of p53 in neural crest and EMT genetic programs, we compared the expression of cell cycle , neural crest and EMT markers by QRT-PCR analysis in mouse embryonic fibroblasts (MEFs) derived from *p53* wt ($p53^{+/+}$) and knockout ($p53^{-/-}$) mice (Fig. 8A,B). MEFs obtained from embryos 13.5 days post-coitum represent a heterogeneous population of primary adherent cells with variable differentiation capacity (Molchadsky et al., 2008). We tested the effect of Nutlin-3 treatment on these MEFs in order to obtain insights into the p53-independent (presumably Mdm2-dependent) effects of this drug. As a positive control, we verified that the classical p53 targets *Mdm2*, *p21* and *Ccng1* are downregulated, whereas *Mycn* is upregulated, in *p53* null as compared with control MEFs (Fig. 8B). Nutlin-3 induced *Mdm2*, *p21* and *Ccng1* expression in the control MEFs but not in *p53* null MEFs, whereas *Mycn* was repressed by Nutlin-3 (Fig. 8B). Consistent with our in vivo data in the chick, the neural crest/EMT markers *Sox9*, *Snail1* and *Snail2* were upregulated in *p53* null MEFs, whereas *Sox10* was reduced (Fig. 8B and Fig. 1). Stabilization of p53 by Nutlin-3 repressed all these genes, including *Twist* and *Zeb2* (data not shown), in line with the idea that p53 antagonizes EMT in the mouse. Taken together, this in vitro analysis supports our finding that loss of p53 facilitates neural crest/EMT gene expression, presumably by affecting cell growth.

## DISCUSSION

Although significant progress has been achieved in understanding the function(s) of p53 in cancer, its role(s) during embryogenesis is far less clear. There is no doubt that p53 is one of the most important proteins in the cell; therefore, its activities during embryogenesis in mammals are masked by diverse, robust redundancy mechanisms. In this study, we used *p53* knockout mouse embryos, as well as dynamic perturbation approaches in chick embryos, to study p53 involvement in neural crest development, with an emphasis on EMT, a key process during embryogenesis and malignant transformation.

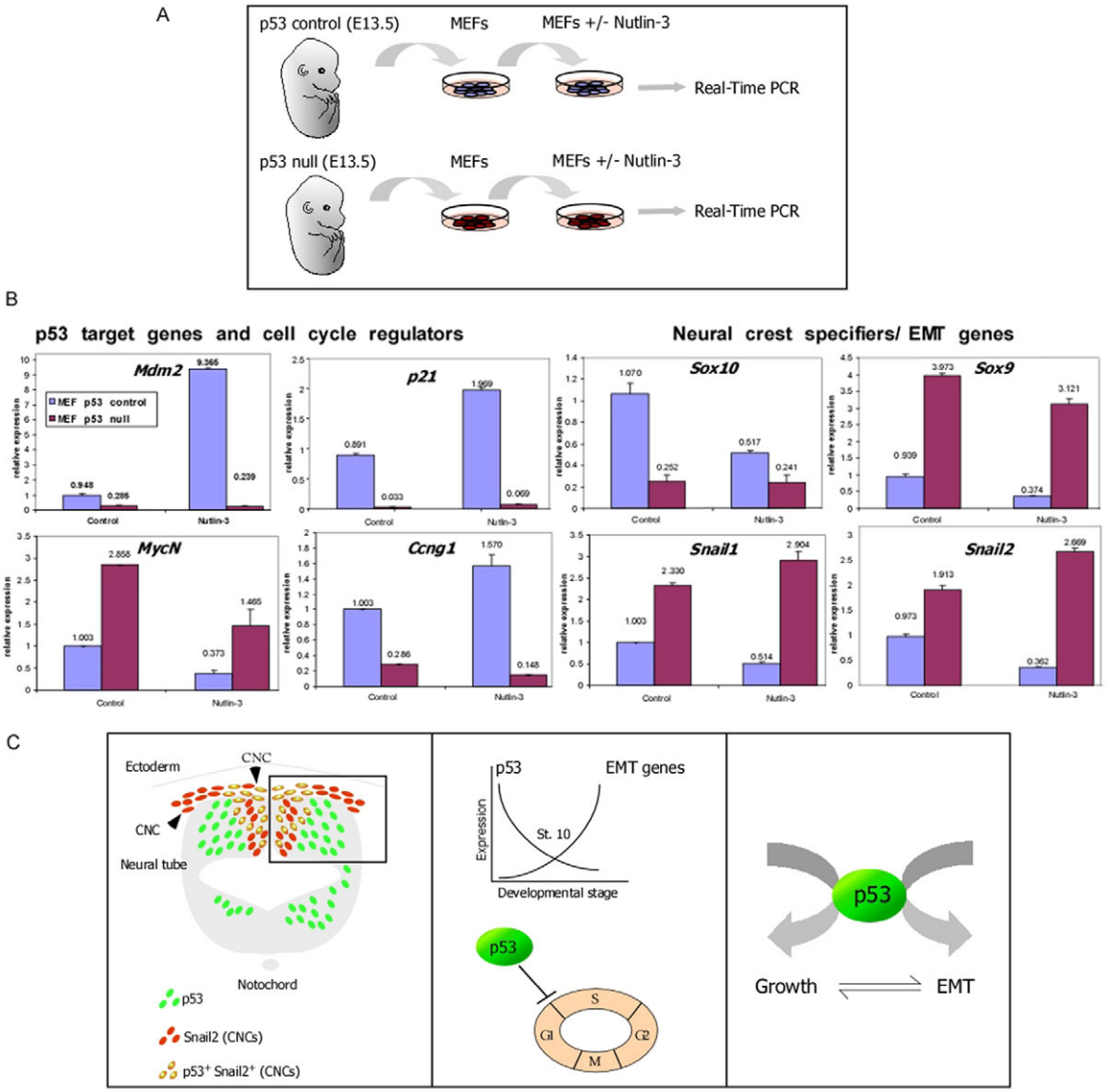


**Fig. 8. p53 controls the neural crest/EMT gene network in mouse embryonic fibroblasts.** (**A**) A scheme describing the mouse embryonic fibroblast (MEF) analysis system used in this paper (see Materials and methods for details). (**B**) QRT-PCR analysis of genes expressed by wt *p53* (control) or *p53* null MEFs with or without Nutlin-3 treatment. Error bars indicate s.e.m. Absolute values are given above each bar. (**C**) (Left) Transverse section of St. 9-10 chick neural tube showing the expression of p53 (green cells) and SNAIL2 (red cells); p53+ SNAIL2+ CNC cells are yellow. (Middle) We find a sharp decrease in p53 expression in CNCs undergoing EMT/delamination. (Right) Modulating p53 levels in the neural tube revealed changes in cell cycle genes and proliferation suggesting that p53 coordinates CNC cell growth and EMT processes during neural tube closure.

Our findings reveal that p53 is downregulated in CNC cells as they undergo EMT. We show that loss of p53 promotes EMT gene expression. In *p53* knockout embryos, broad craniofacial defects are seen. We also provide evidence that p53 exerts its function by regulating cell cycle progression at the onset of CNC EMT/delamination (Fig. 8C). We suggest that p53 regulates a group of neural crest specifiers (Sauka-Spengler and Bronner-Fraser, 2008), such as Snail2, Sox9, Sox10, Pax7, Ets1 and Mycn, that promote neural crest/EMT processes. The strong expression of *MYCN* in CNC progenitors in the chick neural tube might suggest a specific role for this gene in the regulation of CNC cell growth, downstream of p53. Interestingly, Nutlin-3 application to neural crest-derived childhood malignancy neuroblastoma cells, which contain amplified MYCN levels, results in a pronounced anti-proliferative effect (Van Maerken et al., 2006).

Furthermore, p53 may be involved in other important aspects of CNC development, such as population size control of CNC progenitors. Our findings imply that conventional genetic loss-of-function studies in mice might provide an incomplete picture of dynamic biological processes such as those regulated by p53 during vertebrate embryogenesis.

## p53 is expressed by CNC progenitors and is required for proper CNC development

Neural crest precursors in the neural tube undergo dynamic cellular processes within a short developmental window. These cells divide extensively, both symmetrically to maintain their stem cell-like properties (i.e. self-renewal) and asymmetrically to generate specified subpopulations. Moreover, as they proliferate, these cells also undergo EMT, delamination and migration. Based on our

findings and the known functions of p53, we suggest that *p53* acts within a regulatory network that controls CNC cell growth, EMT and delamination (Fig. 8C).

The onset of neural crest delamination varies considerably between the head and trunk of the vertebrate embryo (Burstyn-Cohen et al., 2004; Del Barrio and Nieto, 2004; Theveneau et al., 2007). Snail2 (formally known as Slug) is expressed in cells undergoing EMT and in migrating CNC cells (Del Barrio and Nieto, 2004) (this study). It was shown recently that Ets1, a proto-oncogene that is specifically expressed in CNC cells, works together with Snail2 to promote CNC delamination (Theveneau et al., 2007). We show that p53 is expressed in the neural plate and later in the neural tube, which includes CNC progenitors, although its levels decreased significantly in both populations at later developmental stages. The expression of p53 negatively correlates with that of SNAIL2 and ETS1 (Figs 2 and 3). We show that stabilization of p53 suppresses the expression of these genes. Hence, p53 downregulation in CNC progenitors facilitates expression of SNAIL2 and ETS1, both of which are required for EMT/delamination. These findings suggest that p53 activity must be reduced before EMT/delamination of CNC cells can occur. Notably, EMT is known for its repression of another p53-dependent process, cellular senescence, which is the inability of cells to proliferate in the presence of nutrients and mitogens (d'Adda di Fagagna, 2008).

## p53 regulates CNC cell growth

It is well known that p53 promotes cell cycle arrest. Indeed, decreased p53 expression in the chick neural tube was correlated with an increase in the number of proliferating CNC cells (see Fig. S5 in the supplementary material). Furthermore, nuclear stabilization of p53 by Nutlin-3 induced the expression of *CCNG1*, a p53-responsive gene that inhibits cell growth (Zhao et al., 2003), and suppressed *MYCN*, which is known to promote cell cycle progression (Schweigerer et al., 1990). Likewise, in haploinsufficient mice, *Tcof1* (the gene involved in TCS) leads to nuclear stabilization of the p53 protein, which, in turn, leads to activation of *Ccng1* and cell cycle arrest (as well as to caspase 3-mediated apoptosis) of CNC progenitors (Jones et al., 2008). Thus, we conclude that downregulation of p53 in CNC progenitors is required to prevent cell cycle arrest.

Inactivation of p53 induces excess cell growth, as seen in the case of exencephaly, which is often observed in *p53* null mouse embryos (Armstrong et al., 1995; Sah et al., 1995). Along these lines, we have shown that loss of p53 activity induced by DNp53 results in increased $PAX7^+$ $SOX9^+$ CNC cell numbers (Figs 5 and 6). Taken together, these findings suggest that p53 acts upstream of the cell cycle-related factors Mycn and Ccng1 (Fig. 7), among others, to fine-tune cell growth and EMT/delamination processes (Fig. 8C, right panel). It has been proposed that p53 can inhibit cell proliferation through its role as a negative regulator of ribosome biogenesis (Jones et al., 2008). Intriguingly, the transient activity of p53 in CNC progenitors that we observed in the chick seems to be distinct from the classical p53/p21-dependent pathway.

Blocking p53 activity by DNp53 resulted in severe defects in CNC cell migration (Fig. 6), suggesting that CNC cells cannot properly delaminate and migrate when their growth/proliferation is perturbed. Indeed, evidence for a link between growth control and neural crest delamination/migration has been shown in both frog and chick models (Burstyn-Cohen et al., 2004; Gessert et al., 2007).

## p53-Snail2 regulatory loop

Our results suggest that p53 levels are reduced concomitantly with the upregulation of SNAIL2 and CNC EMT/delamination from the neural tube (Figs 2-4). Recent findings indicate that p53 directly activates Snail2 by binding to its promoter following DNA damage (Wu et al., 2005), whereas Snail2 was shown to bind and repress the E boxes within the cadherin 6B promoter to initiate neural crest EMT/delamination (Taneyhill et al., 2007). Although Snail2 was previously shown to repress p53-mediated apoptosis (Kurrey et al., 2009), in our studies electroporation of *Snail2* had no apparent effect on p53 expression (data not shown). Moreover, a recent study has suggested that Mdm2 is a putative E3 ligase of Snail2, directing it towards proteasomal degradation (Wang et al., 2009). This study suggests a negative relationship between p53 and Snail2 via Mdm2, whereas our findings point to the direct or indirect transcriptional regulation of *Snail2* by p53 (Fig. 4).

Snail2 and p53 play key roles during neural tube closure in many organisms, including humans (Pangilinan et al., 2008; Stegmann et al., 1999). Indeed, we observed a large number of neural tube defects (NTDs) in our experiments (data not shown), in agreement with a role for the p53-Snail2 regulatory loop in such defects. NTDs undoubtedly affect the contribution of CNC cells to different lineages (cartilage, bones, tendons and sensory neurons). Notably, Nutlin-3 treatment did not affect Sox9 or Col2a expression, indicating normal cartilage differentiation. These results might suggest that other CNC-derived populations (e.g. connective tissues) are apparently affected by these manipulations. Furthermore, in the Nutlin-3 experiments we observed that some CNC cells were able to migrate out of the neural tube, despite the downregulation of SNAIL2 (Figs 4 and 6); thus, we speculate that there is a Snail2-independent EMT/delamination mechanism at work in these cells.

## Manipulations of p53 affect craniofacial muscle patterning non-cell autonomously

In recent years, the regulation of head muscle patterning and differentiation by neural crest cells has been a subject of intensive research (Grenier et al., 2009; Heude et al., 2010; Noden and Trainor, 2005; Rinon et al., 2007; Tokita and Schneider, 2009; Tzahor et al., 2003). Our craniofacial muscle analyses in chick and mouse embryos have uncovered global head muscle patterning defects in *p53* KO mice. Because p53 is hardly detected in head muscle progenitors, we conclude that these muscle patterning defects are mediated non-cell autonomously by CNC cells. Future studies should probe p53-related extrinsic mechanisms in specific CNC lineages in order to clarify the cause(s) of these muscle patterning defects. Interestingly, in the chick, Nutlin-3 treatment induced pronounced muscle defects, whereas cartilage markers were less affected. Moreover, we did not observe comparable muscle patterning defects in trunk muscles, highlighting the distinct nature of the head musculature and the important role of CNC cells in head myogenesis.

In conclusion, this study revealed non-apoptotic roles for p53 during early CNC development. These p53-dependent activities affect distinct craniofacial characteristics. We suggest that p53 stands at a nodal point in the control of cell cycle progression and EMT/delamination. Obviously, these two cellular processes are not mutually exclusive, but must be tightly coordinated during embryogenesis, as well as in tumorigenesis.

**Acknowledgements**

We thank Ayelet Jerafi for technical help and Prof. Lozano (MD Anderson Cancer Center, University of Texas) for insightful discussions and sharing data. E.T. is the incumbent of the Gertrude and Philip Nollman Career Development

Chair. This work was supported by research grants to E.T. from the Helen and Martin Kimmel Institute for Stem Cell Research, the Minerva Foundation, the Association Française Contre les Myopathies, the Israel Science Foundation, the German-Israel Foundation (GIF) and the United States-Israel Binational Science Foundation.

**Competing interests statement**
The authors declare no competing financial interests.

**Supplementary material**
Supplementary material for this article is available at
http://dev.biologists.org/lookup/suppl/doi:10.1242/dev.053645/-/DC1

**References**

**Acloque, H., Adams, M. S., Fishwick, K., Bronner-Fraser, M. and Nieto, M. A.** (2009). Epithelial-mesenchymal transitions: the importance of changing cell state in development and disease. *J. Clin. Invest.* **119**, 1438-1449.
**Almog, N. and Rotter, V.** (1997). Involvement of p53 in cell differentiation and development. *Biochim. Biophys. Acta* **1333**, F1-F27.
**Armstrong, J. F., Kaufman, M. H., Harrison, D. J. and Clarke, A. R.** (1995). High-frequency developmental abnormalities in p53-deficient mice. *Curr. Biol.* **5**, 931-936.
**Burstyn-Cohen, T., Stanleigh, J., Sela-Donenfeld, D. and Kalcheim, C.** (2004). Canonical Wnt activity regulates trunk neural crest delamination linking BMP/noggin signaling with G1/S transition. *Development* **131**, 5327-5339.
**Cam, H., Griesmann, H., Beitzinger, M., Hofmann, L., Beinoraviciute-Kellner, R., Sauer, M., Huttinger-Kirchhof, N., Oswald, C., Friedl, P., Gattenlohner, S. et al.** (2006). p53 family members in myogenic differentiation and rhabdomyosarcoma development. *Cancer Cell* **10**, 281-293.
**Cordenonsi, M., Dupont, S., Maretto, S., Insinga, A., Imbriano, C. and Piccolo, S.** (2003). Links between tumor suppressors: p53 is required for TGF-beta gene responses by cooperating with Smads. *Cell* **113**, 301-314.
**d'Adda di Fagagna, F.** (2008). Cellular senescence and cellular longevity: nearly 50 years on and still working on it. *Exp. Cell Res.* **314**, 1907-1908.
**Daujat, S., Neel, H. and Piette, J.** (2001). Preferential expression of Mdm2 oncogene during the development of neural crest and its derivatives in mouse early embryogenesis. *Mech. Dev.* **103**, 163-165.
**Del Barrio, M. G. and Nieto, M. A.** (2004). Relative expression of Slug, RhoB, and HNK-1 in the cranial neural crest of the early chicken embryo. *Dev. Dyn.* **229**, 136-139.
**Donehower, L. A., Harvey, M., Slagle, B. L., McArthur, M. J., Montgomery, C. A., Jr, Butel, J. S. and Bradley, A.** (1992). Mice deficient for p53 are developmentally normal but susceptible to spontaneous tumours. *Nature* **356**, 215-221.
**Gessert, S., Maurus, D., Rossner, A. and Kuhl, M.** (2007). Pescadillo is required for Xenopus laevis eye development and neural crest migration. *Dev. Biol.* **310**, 99-112.
**Grenier, J., Teillet, M. A., Grifone, R., Kelly, R. G. and Duprez, D.** (2009). Relationship between neural crest cells and cranial mesoderm during head muscle development. *PLoS One* **4**, e4381.
**Hamburger, V. and Hamilton, H. L.** (1992). A series of normal stages in the development of the chick embryo. 1951. *Dev. Dyn.* **195**, 231-272.
**Harel, I., Nathan, E., Tirosh-Finkel, L., Zigdon, H., Guimaraes-Camboa, N., Evans, S. M. and Tzahor, E.** (2009). Distinct origins and genetic programs of head muscle satellite cells. *Dev. Cell* **16**, 822-832.
**Helms, J. A., Cordero, D. and Tapadia, M. D.** (2005). New insights into craniofacial morphogenesis. *Development* **132**, 851-861.
**Heude, E., Bouhali, K., Kurihara, Y., Kurihara, H., Couly, G., Janvier, P. and Levi, G.** (2010). Jaw muscularization requires Dlx expression by cranial neural crest cells. *Proc. Natl. Acad. Sci. USA* **107**, 11441-11446.
**Hong, C. S. and Saint-Jeannet, J. P.** (2005). Sox proteins and neural crest development. *Semin. Cell Dev. Biol.* **16**, 694-703.
**Jones, N. C., Lynn, M. L., Gaudenz, K., Sakai, D., Aoto, K., Rey, J. P., Glynn, E. F., Ellington, L., Du, C., Dixon, J. et al.** (2008). Prevention of the neurocristopathy Treacher Collins syndrome through inhibition of p53 function. *Nat. Med.* **14**, 125-133.
**Krinka, D., Raid, R., Pata, I., Karner, J. and Maimets, T.** (2001). In situ hybridisation of chick embryos with p53-specific probe and their immunostaining with anti-p53 antibodies. *Anat. Embryol. (Berl.)* **204**, 207-215.
**Kurrey, N. K., Jalgaonkar, S. P., Joglekar, A. V., Ghanate, A. D., Chaskar, P. D., Doiphode, R. Y. and Bapat, S. A.** (2009). Snail and slug mediate radioresistance and chemoresistance by antagonizing p53-mediated apoptosis and acquiring a stem-like phenotype in ovarian cancer cells. *Stem Cells* **27**, 2059-2068.
**Lane, D. P.** (1992). Cancer. p53, guardian of the genome. *Nature* **358**, 15-16.
**Le Douarin, N. and Kalcheim, C.** (1999). *The Neural Crest.* Cambridge, UK: Cambridge University Press.
**Molchadsky, A., Shats, I., Goldfinger, N., Pevsner-Fischer, M., Olson, M., Rinon, A., Tzahor, E., Lozano, G., Zipori, D., Sarig, R. et al.** (2008). p53 plays a role in mesenchymal differentiation programs, in a cell fate dependent manner. *PLoS One* **3**, e3707.
**Morgan, S. C., Lee, H. Y., Relaix, F., Sandell, L. L., Levorse, J. M. and Loeken, M. R.** (2008). Cardiac outflow tract septation failure in Pax3-deficient embryos is due to p53-dependent regulation of migrating cardiac neural crest. *Mech. Dev.* **125**, 757-767.
**Nathan, E., Monovich, A., Tirosh-Finkel, L., Harrelson, Z., Rousso, T., Rinon, A., Harel, I., Evans, S. M. and Tzahor, E.** (2008). The contribution of Islet1-expressing splanchnic mesoderm cells to distinct branchiomeric muscles reveals significant heterogeneity in head muscle development. *Development* **135**, 647-657.
**Nieto, M. A.** (2002). The snail superfamily of zinc-finger transcription factors. *Nat. Rev. Mol. Cell Biol.* **3**, 155-166.
**Noden, D. M.** (1983a). The embryonic origins of avian cephalic and cervical muscles and associated connective tissues. *Am. J. Anat.* **168**, 257-276.
**Noden, D. M.** (1983b). The role of the neural crest in patterning of avian cranial skeletal, connective, and muscle tissues. *Dev. Biol.* **96**, 144-165.
**Noden, D. M. and Trainor, P. A.** (2005). Relations and interactions between cranial mesoderm and neural crest populations. *J. Anat.* **207**, 575-601.
**Ossovskaya, V. S., Mazo, I. A., Chernov, M. V., Chernova, O. B., Strezoska, Z., Kondratov, R., Stark, G. R., Chumakov, P. M. and Gudkov, A. V.** (1996). Use of genetic suppressor elements to dissect distinct biological effects of separate p53 domains. *Proc. Natl. Acad. Sci. USA* **93**, 10309-10314.
**Pangilinan, F., Geiler, K., Dolle, J., Troendle, J., Swanson, D. A., Molloy, A. M., Sutton, M., Conley, M., Kirke, P. N., Scott, J. M. et al.** (2008). Construction of a high resolution linkage disequilibrium map to evaluate common genetic variation in TP53 and neural tube defect risk in an Irish population. *Am. J. Med. Genet.* **146A**, 2617-2625.
**Pani, L., Horal, M. and Loeken, M. R.** (2002). Rescue of neural tube defects in Pax-3-deficient embryos by p53 loss of function: implications for Pax-3-dependent development and tumorigenesis. *Genes Dev.* **16**, 676-680.
**Porrello, A., Cerone, M. A., Coen, S., Gurtner, A., Fontemaggi, G., Cimino, L., Piaggio, G., Sacchi, A. and Soddu, S.** (2000). p53 regulates myogenesis by triggering the differentiation activity of pRb. *J. Cell Biol.* **151**, 1295-1304.
**Rinon, A., Lazar, S., Marshall, H., Buchmann-Moller, S., Neufeld, A., Elhanany-Tamir, H., Taketo, M. M., Sommer, L., Krumlauf, R. and Tzahor, E.** (2007). Cranial neural crest cells regulate head muscle patterning and differentiation during vertebrate embryogenesis. *Development* **134**, 3065-3075.
**Sah, V. P., Attardi, L. D., Mulligan, G. J., Williams, B. O., Bronson, R. T. and Jacks, T.** (1995). A subset of p53-deficient embryos exhibit exencephaly. *Nat. Genet.* **10**, 175-180.
**Sasai, N., Yakura, R., Kamiya, D., Nakazawa, Y. and Sasai, Y.** (2008). Ectodermal factor restricts mesoderm differentiation by inhibiting p53. *Cell* **133**, 878-890.
**Sauka-Spengler, T. and Bronner-Fraser, M.** (2008). A gene regulatory network orchestrates neural crest formation. *Nat. Rev. Mol. Cell Biol.* **9**, 557-568.
**Schwarzkopf, M., Coletti, D., Sassoon, D. and Marazzi, G.** (2006). Muscle cachexia is regulated by a p53-PW1/Peg3-dependent pathway. *Genes Dev.* **20**, 3440-3452.
**Schweigerer, L., Breit, S., Wenzel, A., Tsunamoto, K., Ludwig, R. and Schwab, M.** (1990). Augmented MYCN expression advances the malignant phenotype of human neuroblastoma cells: evidence for induction of autocrine growth factor activity. *Cancer Res.* **50**, 4411-4416.
**Shoval, I., Ludwig, A. and Kalcheim, C.** (2007). Antagonistic roles of full-length N-cadherin and its soluble BMP cleavage product in neural crest delamination. *Development* **134**, 491-501.
**Soddu, S., Blandino, G., Scardigli, R., Coen, S., Marchetti, A., Rizzo, M. G., Bossi, G., Cimino, L., Crescenzi, M. and Sacchi, A.** (1996). Interference with p53 protein inhibits hematopoietic and muscle differentiation. *J. Cell Biol.* **134**, 193-204.
**Stegmann, K., Boecker, J., Kosan, C., Ermert, A., Kunz, J. and Koch, M. C.** (1999). Human transcription factor SLUG: mutation analysis in patients with neural tube defects and identification of a missense mutation (D119E) in the Slug subfamily-defining region. *Mutat. Res.* **406**, 63-96.
**Stiewe, T.** (2007). The p53 family in differentiation and tumorigenesis. *Nat. Rev. Cancer* **7**, 165-168.
**Tajbakhsh, S., Rocancourt, D. and Buckingham, M.** (1996). Muscle progenitor cells failing to respond to positional cues adopt non-myogenic fates in myf-5 null mice. *Nature* **384**, 266-270.
**Taneyhill, L. A., Coles, E. G. and Bronner-Fraser, M.** (2007). Snail2 directly represses cadherin6B during epithelial-to-mesenchymal transitions of the neural crest. *Development* **134**, 1481-1490.
**Theveneau, E., Duband, J. L. and Altabef, M.** (2007). Ets-1 confers cranial features on neural crest delamination. *PLoS One* **2**, e1142.
**Tirosh-Finkel, L., Elhanany, H., Rinon, A. and Tzahor, E.** (2006). Mesoderm progenitor cells of common origin contribute to the head musculature and the cardiac outflow tract. *Development* **133**, 1943-1953.
**Tokita, M. and Schneider, R. A.** (2009). Developmental origins of species-specific muscle pattern. *Dev. Biol.* **331**, 311-325.

**Trainor, P. A. and Tam, P. P.** (1995). Cranial paraxial mesoderm and neural crest cells of the mouse embryo: co-distribution in the craniofacial mesenchyme but distinct segregation in branchial arches. *Development* **121**, 2569-2582.
**Trainor, P. A. and Krumlauf, R.** (2001). Hox genes, neural crest cells and branchial arch patterning. *Curr. Opin. Cell Biol.* **13**, 698-705.
**Tucker, G. C., Duband, J. L., Dufour, S. and Thiery, J. P.** (1988). Cell-adhesion and substrate-adhesion molecules: their instructive roles in neural crest cell migration. *Development* **103 Suppl**, 81-94.
**Tzahor, E.** (2009). Heart and craniofacial muscle development: a new developmental theme of distinct myogenic fields. *Dev. Biol.* **334**, 513-522.
**Tzahor, E., Kempf, H., Mootoosamy, R. C., Poon, A. C., Abzhanov, A., Tabin, C. J., Dietrich, S. and Lassar, A. B.** (2003). Antagonists of Wnt and BMP signaling promote the formation of vertebrate head muscle. *Genes Dev.* **17**, 3087-3099.
**Van Maerken, T., Speleman, F., Vermeulen, J., Lambertz, I., De Clercq, S., De Smet, E., Yigit, N., Coppens, V., Philippe, J., De Paepe, A. et al.** (2006). Small-molecule MDM2 antagonists as a new therapy concept for neuroblastoma. *Cancer Res.* **66**, 9646-9655.
**Vassilev, L. T.** (2007). MDM2 inhibitors for cancer therapy. *Trends Mol. Med.* **13**, 23-31.
**Wang, S. P., Wang, W. L., Chang, Y. L., Wu, C. T., Chao, Y. C., Kao, S. H., Yuan, A., Lin, C. W., Yang, S. C., Chan, W. K. et al.** (2009). p53 controls cancer cell invasion by inducing the MDM2-mediated degradation of Slug. *Nat. Cell Biol.* **11**, 694-704.
**Wu, W. S., Heinrichs, S., Xu, D., Garrison, S. P., Zambetti, G. P., Adams, J. M. and Look, A. T.** (2005). Slug antagonizes p53-mediated apoptosis of hematopoietic progenitors by repressing puma. *Cell* **123**, 641-653.
**Yang, J. and Weinberg, R. A.** (2008). Epithelial-mesenchymal transition: at the crossroads of development and tumor metastasis. *Dev. Cell* **14**, 818-829.
**Zambetti, G. P., Horwitz, E. M. and Schipani, E.** (2006). Skeletons in the p53 tumor suppressor closet: genetic evidence that p53 blocks bone differentiation and development. *J. Cell Biol.* **172**, 795-797.
**Zhao, L., Samuels, T., Winckler, S., Korgaonkar, C., Tompkins, V., Horne, M. C. and Quelle, D. E.** (2003). Cyclin G1 has growth inhibitory activity linked to the ARF-Mdm2-p53 and pRb tumor suppressor pathways. *Mol. Cancer Res.* **1**, 195-206.